Colloids and Surfaces B: Biointerfaces 181 (2019) 48–57

Contents lists available at ScienceDirect

Colloids and Surfaces B: Biointerfaces

journal homepage: www.elsevier.com/locate/colsurfb

Effects of carbon dots surface functionalities on cellular behaviors – Mechanistic exploration for opportunities in manipulating uptake and translocation

Gui-Hua Yan[a], Zheng-Mei Song[a], Yuan-Yuan Liu[a], Qianqian Su[a], Weixiong Liang[b], Aoneng Cao[a], Ya-Ping Sun[b,*], Haifang Wang[a,*]

[a] Institute of Nanochemistry and Nanobiology, Shanghai University, Shanghai 200444, China
[b] Department of Chemistry and Laboratory for Emerging Materials and Technology, Clemson University, Clemson, SC, 29634, USA

ARTICLE INFO

Keywords:
Carbon dots
Surface passivation
Cellular uptake
Cell cycle
Translocation

ABSTRACT

Carbon dots (CDots) for their excellent optical and other properties have been widely pursued for potential biomedical applications, in which a more comprehensive understanding on the cellular behaviors and mechanisms of CDots is required. For such a purpose, two kinds of CDots with surface passivation by 3-ethoxypropylamine (EPA-CDots) and oligomeric polyethylenimine (PEI-CDots) were selected for evaluations on their uptakes by human cervical carcinoma HeLa cells at three cell cycle phases (G_0/G_1, S and G_2/M), and on their different internalization pathways and translocations in cells. The results show that HeLa cells could internalize both CDots by different pathways, with an overall slightly higher internalization efficiency for PEI-CDots. The presence of serum in culture media could have major effects, significantly enhancing the cellular uptake of EPA-CDots, yet markedly inhibiting that of PEI-CDots. The HeLa cells at different cell cycle phases have different behaviors in taking up the CDots, which are also affected by the different dot surface moieties and serum in culture media. Mechanistic implications of the results and the opportunities associated with an improved understanding on the cellular behaviors of CDots for potentially the manipulation and control of their cellular uptakes and translocations are discussed.

1. Introduction

As newly established fluorescence nanoprobes, fluorescent semiconductor nanocrystals, commonly referred to as quantum dots (QDs), have been used to replace organic dyes and also in some applications genetically encoded fluorescent tags for major advantages such as the fluorescence brightness at the individual dot level, photostability, and others [1–3]. For both the growing demand on high-performance fluorescence probes and the need to address some serious shortcomings of the established semiconductor QDs, especially with respect to their known toxicities, much effort has been made to expand the offering of QD-like fluorescent nanomaterials beyond those based on conventional semiconductors. In this regard, carbon dots (CDots) have emerged to represent a performance-wise competitive yet benign and nontoxic alternative [4–6], and the broad appeal of these zero-dimensional carbon-based nanomaterials of bright and colorful fluorescence emissions to the research community is made evident by the large and even increasing number of relevant publications in the recent literature [6,7].

CDots are generally defined as small carbon nanoparticles with various surface passivation schemes [4,6,8]. Structurally more closely adhering to the definition are the CDots prepared from pre-existing carbon nanoparticles with deliberate particle surface chemical functionalization by selected organic molecules [4,9]. These CDots have strong fluorescence in the green spectral region [9,10], the same region for the emission of green fluorescence proteins [9–11], and their promise in fluorescence tagging and imaging of cells was already demonstrated in the initial finding of CDots [4]. Nevertheless, in addition to these CDots for cell imaging and related investigations [12], there have been many syntheses mostly based on “one-pot” carbonization of various organic precursors for CDots or the like to be used for cell imaging and other cellular studies [12–15]. For example, Shuang et al. reported subcellular targeting features of surface regulated CDots, with the dots of surface amine moieties targeting lysosome and those of laurylamine on the dot surface residing in endoplasmic reticulum in cells [14].

Generally for CDots as a new class of nanoscale fluorescence probes, most reported investigations have been limited to their toxicity profiles

* Corresponding authors.
E-mail addresses: syaping@clemson.edu (Y.-P. Sun), hwang@shu.edu.cn (H. Wang).

https://doi.org/10.1016/j.colsurfb.2019.05.027
Received 16 February 2019; Received in revised form 23 April 2019; Accepted 14 May 2019
Available online 14 May 2019
0927-7765/

in cells or simple demonstrations on their being able to enter cells or serving as fluorescence tags for cells. Yet, many of the potential applications of CDots, such as those for bioimaging, drug delivery, specific targeting, therapeutic assessments, and so on, require a more comprehensive and in-depth understanding of their cellular behaviors, including details on interactions between CDots and cells, endocytosis mechanisms, intra-cellular distributions of CDots and their evolution over time, among others.

In the work reported here, we used human cervical carcinoma HeLa cell line as a cell model to systematically study the cellular uptake and translocation of CDots with two different surface passivation molecules, 3-ethoxypropylamine (EPA-CDots) versus oligomeric polyethylenimine (PEI-CDots), both of which were prepared by the deliberate chemical functionalization of pre-processed and selected small carbon nanoparticles. The results suggested that both kinds of CDots could be internalized by the cells and translocated to lysosomes. However, the internalization processes were significantly different between the two kinds of CDots due to their different surface moieties, and the processes were also clearly influenced by the cycle phase of cells and the presence of serum in culture media. Mechanistic implications of the findings and the opportunities associated with an improved understanding on the cellular behaviors of CDots for potentially the manipulation and control of their cellular uptakes and translocations are discussed.

2. Experimental section

2.1. Measurement

UV/vis absorption spectra were recorded on a Shimadzu UV2501 spectrophotometer. Fluorescence spectra were acquired on a Jobin-Yvon emission spectrometer equipped with a 450 W xenon source, Gemini-180 excitation and Triax-550 emission monochromators, and a photon counting detector (Hamamatsu R928P PMT at 950 V). Fourier-transform infrared (FT-IR) spectra were acquired on a Perkin Elmer Spectrum Two spectrometer. High-resolution transmission electron microscopy (HRTEM) imaging was performed on a JEM-2100 F instrument (JEOL, Japan).

2.2. Carbon dots

Small carbon nanoparticles were harvested from the commercially acquired carbon nano-powders (US Research Nanomaterials, Inc.) in procedures similar to those reported previously [10,16]. EPA-CDots and PEI-CDots were prepared by functionalizing the small carbon nanoparticles with EPA and oligomeric PEI (molecular weight ˜1200) in the same procedures and under the same conditions as ref. 10 and ref. 16, respectively.

Solutions of the CDots with concentrations of 20 μg/mL and 2 μg/mL were used for recording the UV/vis absorption spectra and fluorescence spectra, respectively.

2.3. Cell line and cell culture

HeLa cells (human cervical carcinoma cells) were purchased from the Cell Bank of Type Culture Collection of Chinese Academy of Sciences (Shanghai, China). The cells were cultured in high-glucose DMEM (4.5 g/L glucose) supplemented with 1% penicillin/streptomycin and with/without 10% FBS (fetal bovine serum, Sigma-Aldrich). The cells were cultured in a humidified atmosphere with 5% CO_2 and 95% air at 37 °C.

2.4. Cell viability assay

WST-8 cell counting kit (CCK-8; Dojindo Molecular Technologies Inc., Kumamoto, Japan) was used to evaluate the viability of cells treated with CDots. HeLa cells (5,000/well for the 24 h exposure and 8,000/well for the 2 h exposure) were seeded into 96-well plates and cultured overnight. Then, the cells were exposed to fresh culture media containing CDots. The final concentrations of EPA-CDots were 2.5, 5, 10, 20 and 40 μg/mL, and those of PEI-CDots were 5, 10 and 20 μg/mL. The cells cultured in the media without CDots were used as the control. After 2 h or 24 h, the culture media were abandoned, and the absorbance of the cells treated with or without CDots was measured at 450 nm. The agreement in observed absorbance values suggested that the internalized CDots did not interfere with the CCK-8 assay. Then, CCK-8 solution (100 μL, containing 10% WST-8) was added. After incubation for about 0.5 h, the optical density (OD) of each well at 450 nm was recorded on a microplate reader (Thermo, Varioskan Flash, Waltham, MA, USA). The cell viability (% of control) is expressed as the percentage of $(OD_{test}\text{-}OD_{blank})/(OD_{control}\text{-}OD_{blank})$, where OD_{test} is OD of cells exposed to CDots, $OD_{control}$ is OD of the control, and OD_{blank} is OD of the well without cells.

2.5. Cell synchronization

HeLa cells were synchronized to G_0/G_1 phase, S phase or G_2/M phase by thymidine (TdR) double blocking method. The cell cycle synchronization rates were analyzed by flow cytometry. The details are provided in Supporting Information.

2.6. Cellular uptake

HeLa cells (1×10^5 cells per well) were seeded in 6-well plates and incubated overnight. Then, the cells were synchronized to G_0/G_1 phase, S phase or G_2/M phase. After that, 1 mL of fresh media containing 40 μg/mL EPA-CDots or 10 μg/mL PEI-CDots was introduced to the normal cells, or the cells at different phases. The cells cultured in the media without nanoparticles were set as the control. After 2 h incubation, the cells were washed twice with ice-cold D-Hanks, trypsinized, suspended in media, and then analyzed by flow cytometry. The green fluorescence produced by excitation at 488 nm was recorded.

2.7. Cellular uptake mechanism

After synchronized to G_0/G_1 phase, S phase or G_2/M phase, the cells were incubated at 4 °C or 37 °C (control) for 30 min before incubating with CDots at the same temperature for 2 h. Then, the media were removed and the cells were detected by flow cytometry. The green fluorescence spectra under 488 nm excitation were recorded.

For endocytosis inhibition experiments, HeLa cells were pretreated with media containing an inhibitor involving 7 μg/mL CPZ, 5 μg/mL nocodazole, or 2.5 μg/mL Filipin III before exposure to CDots. After 30 min, the media were removed and a fresh media containing the same inhibitor plus 40 μg/mL EPA-CDots or 10 μg/mL PEI-CDots were added to the cells. After 2 h incubation, the media were removed and the cells were detected by flow cytometry.

2.8. Cellular localization of CDots

HeLa cells (2×10^4 cells per well) were seeded in the Lab-tek™ chamber cover glass (4 holes) and incubated overnight. After the cells were synchronized to G_0/G_1, S and G_2/M phases, fresh media (10% FBS) containing 40 μg/mL of EPA-CDots or 10 μg/mL of PEI-CDots were introduced to the cells. After incubation for 2 h, the media were discarded and D-Hanks buffer containing 100 nM of LysoTracker-Red DND-99 (excitation at 540 nm and emission at 590 nm) or 100 nM of MitoTracker-Red CMXRos (excitation at 540 nm and emission at 590 nm) was introduced to the wells. After 30 min, the supernatants were discarded, and the cells were washed with cold D-Hanks buffer. Finally, 100 μL of media was added, and the cells were investigated and imaged under a confocal laser scanning microscope (Olympus FM 1000, Japan).

For the investigation on the location of CDots in normal HeLa cells, the cells (6×10^4 cells per well) were seeded in the Lab-tek^{TM} chamber cover glass (4 holes). After incubated overnight, 0.5 mL of fresh media containing 40 μg/mL of EPA-CDots or 10 μg/mL of PEI-CDots was added to the cells and cultured for 2 h or 6 h, respectively. Then, lysosomes and mitochondria of cells were labeled, and the cells were imaged under a confocal laser scanning microscope by following the same procedures described above.

2.9. Statistical analysis

The data are expressed as mean ± standard deviation (SD) and all means were calculated from at least three independent experiments. Statistical analysis was performed using the Student t-test. The statistical difference was considered significant when p value < 0.05.

3. Results and discussion

3.1. Carbon dots

Two kinds of CDots samples including EPA-CDots (EPA = 3-ethoxypropylamine) and PEI-CDots (PEI = oligomeric polyethylenimine of an average molecular weight ~1200) were selected for cellular experiments in this study. These samples were prepared and characterized by following the previously reported procedures and techniques [10,16]. The characterization results including those from optical spectroscopy, atomic force microscopy (AFM), transmission electron microscopy (TEM), nuclear magnetic resonance (NMR), and FT-IR (Fig. S1 in Supporting Information) indicated the dots we obtained consisted of small carbon nanoparticle core functionalized by EPA or PEI molecules [10,16]. The two kinds of CDots are both readily soluble in water to form colored homogeneous solutions. The optical absorption and fluorescence spectra of the EPA-CDots and PEI-CDots in aqueous solutions are shown in Fig. 1, and the corresponding fluorescence quantum yields were estimated to be 19% and 10%, respectively. According to results from high resolution TEM analyses (Fig. 2), the EPA-CDots and PEI-CDots are on average 5.2 nm and 6.1 nm in diameter, respectively.

3.2. Cellular uptake of the CDots

CDots are generally benign to cells [5,12], without any severe cytotoxicity found for CDots that are similar to those used in this study [17]. Nevertheless, before the cellular uptake study, effects of the CDots samples on the cell viabilities of HeLa cells were evaluated at different

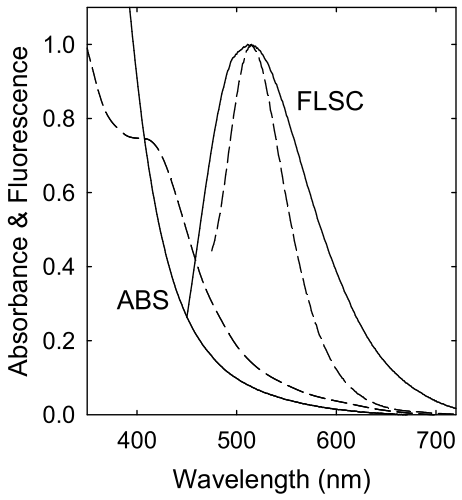

Fig. 1. Absorption (ABS) and fluorescence (FLSC, 440 nm excitation) spectra of EPA-CDots (dashed lines) and PEI-CDots (solid lines) in aqueous solution.

dot concentrations to confirm the nontoxic nature of these CDots. The standard cell viability assay (CCK-8) probing the mitochondrial activity of cells was applied to HeLa cells treated with the CDots. As shown in Fig. 3, the EPA-CDots exhibited no toxicity to the cells across the entire dot concentration range. The cell viability was still above 90% even with the cells exposed to EPA-CDots at the highest concentration of 40 μg/mL for 24 h (Fig. 3A). However, PEI-CDots were more toxic to the cells at higher dot concentrations and more so with a longer exposure time (Fig. 3B). Thus, the concentration of the PEI-CDots at 10 μg/mL was used in all cellular uptake experiments.

Next, flow cytometry was adopted to quantify the cellular uptake of the CDots. HeLa cells were incubated with the CDots for 2 h in culture media with/without serum, and the mean fluorescence intensities (MFI) of a large number of the treated cells were analyzed by flow cytometry. The MFI of cells was used to reflect the uptake of the CDots by HeLa cells (Fig. 4). The higher the value of MFI of cells was, the more CDots were internalized by the cells [18,19].

As reported in the literature [20,21], the presence of serum in media would usually decrease the cellular uptake of nanomaterials. Recently, several reports have also been indicated that the cell cycle may be a factor influencing the cellular uptake [22–25]. In this study, we investigated the effects of both the serum in media and the cell cycle on the uptake of the CDots by HeLa cells. In general, cells proliferate via mitosis and thus go through a complete cell cycle from the end of a division to the end of the next division along phases of G_0/G_1 to S to G_2/M repeatedly. With use of the thymidine (TdR) double blocking method, HeLa cells could be selectively synchronized to the G_0/G_1 phase, S phase, or G_2/M phase. In our experiments we achieved a synchronization rate of 88.97% for G_0/G_1, 84.39% for S, and 61.57% for G_2/M (Fig. S2 and Table S1). These results are comparable with those reported in the literature [24]. Since cells grow continuously, namely the cell cycle continues, the synchronized cells may grow in different speeds and then gradually enter different phases, which would allow an estimate on how long the synchronized cells remain at the targeted phase. Our results suggested that the synchronized cells could stay at their own phase for more than 2 h (Fig. S3). More details on the cell synchronization are provided in Supporting Information. As shown in Fig. 4, the results on the cellular uptake of the CDots by normal HeLa cells and the cells at the different phases were summarized. Apparently, both kinds of CDots could be internalized by HeLa cells, with or without the presence of serum in media. More quantitatively, however, it is interesting that serum enhances the cellular uptake of EPA-CDots (Fig. 4A), yet hinders that of PEI-CDots (Fig. 4B), regardless of any cell synchronization.

For the cells at different phases, their abilities of internalizing the CDots were different, and the degree of the difference was somewhat dependent on the presence of serum. With or without the serum, the uptakes of EPA-CDots by the phase G_2/M and phase S cells were comparable (Fig. 4A), and they were both higher than that by the phase G_0/G_1 cells (Fig. 4A), but the difference was smaller in the absence of serum, suggesting that the serum could affect the uptakes by the cells at different phases. The results on the uptakes of PEI-CDots were similar in the presence of serum (Fig. 4B). However, in serum-free media, cells at the S phase had the highest uptakes of PEI-CDots, followed by cells at the G_0/G_1 phase, and the least by cells at the G_2/M phase. As reported in the literature [20,21,23], the uptake of nanoparticles by cells in different phases generally follows the trend of $G_2/M > S > G_0/G_1$. Apparently, such a trend is applicable to the uptake of EPA-CDots. For PEI-CDots, however, the same trend can be found only in the presence of serum, obviously not in serum-free media (Fig. 4).

The different behaviors of EPA-CDots and PEI-CDots in the cellular uptake in serum-free media (Fig. 4) are likely due primarily to the different characteristics of the dot surface moieties between the two CDots. PEI is generally considered as being cationic for the fact that amine groups in the molecule are protonated at physiological pH (D-Hanks buffer in this study), as oligomeric or polymeric PEI is commonly

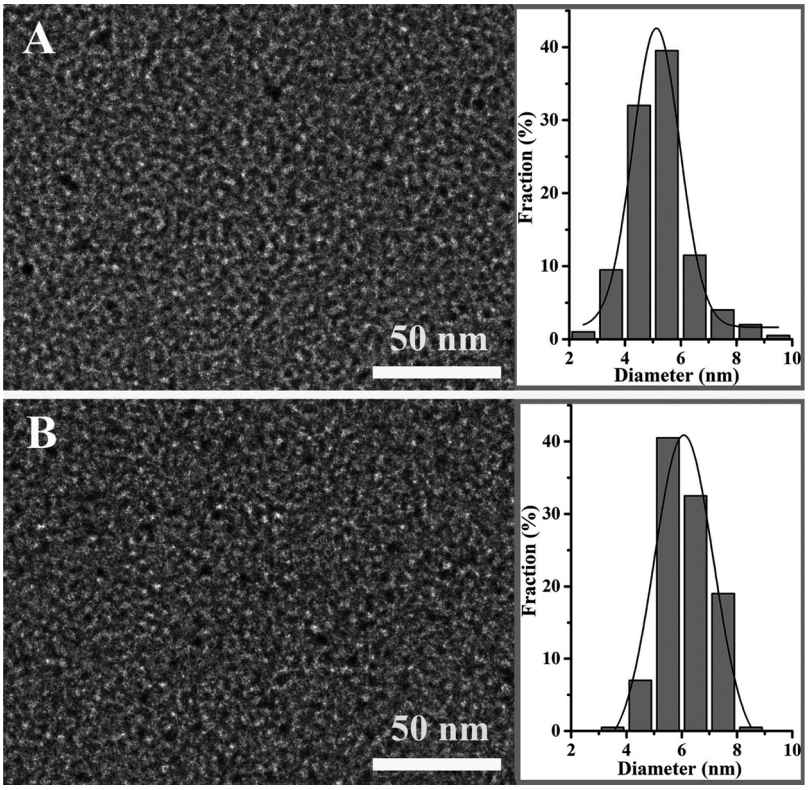

Fig. 2. Representative TEM images and size distributions of EPA-CDots (A) and PEI-CDots (B).

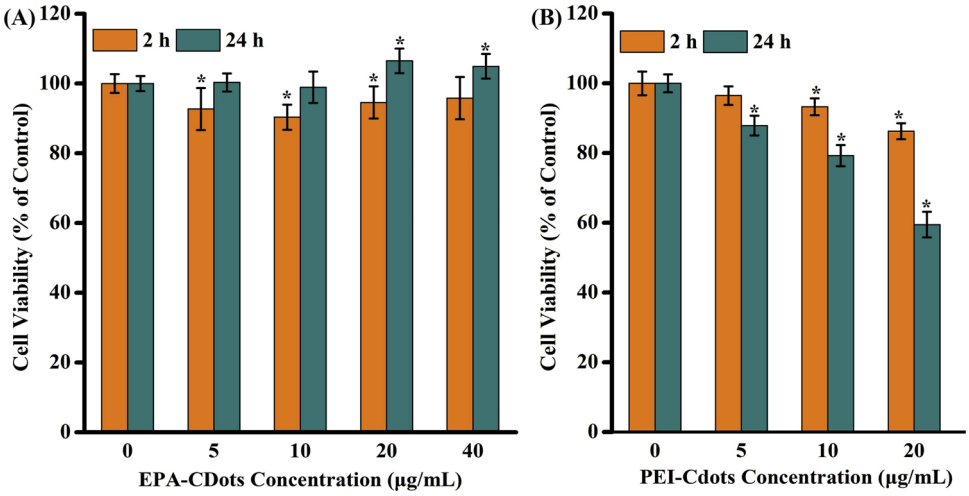

Fig. 3. Viabilities of HeLa cells after exposure to EPA-CDots (A) and PEI-CDots (B) for 2 h or 24 h. *$p < 0.05$ compared with the control (0 μg/mL) (n = 6).

used in gene transfection for improved efficiency [13,26]. There have also been reports on the ability of PEI in cell adhesion and their applications for enhanced membrane permeability to facilitate easier cell entry [27]. In media containing serum, the cellular uptake of PEI-CDots was overall lower, probably due to the adsorption of proteins resulting in the formation of a protein corona on the dot surface, which would impede the entry of PEI-CDots into cells. However, such a rationale may not be consistent with the observation that EPA-CDots cultured in media with serum exhibited higher cellular uptake than that in serum-free media. More investigations are necessary for an improved mechanistic understanding of these very interesting results.

For cells at the different phases in media with serum, the lowest uptake of both CDots was found at the G_0/G_1 phase or G_2/M phase, and the highest at the S phase (Fig. 4). The lowest uptake at the G_0/G_1 phase is consistent with the previously reported studies [22,23,28]. On the latter, Kim, et al. reported that in the internalization of carboxyl polystyrene nanoparticles by A549 cells, the highest uptake was at the G_2/M phase [23]. However, in their study, cellular uptake efficiencies were determined after the nanoparticles were interacted with the synchronized cells for 24 h. Since synchronized cells could only maintain for a short period of time (2–4 h see also Fig. S3 in Supporting Information) [29,30], the 24 h time period used in their study was likely much too long to reflect accurately the behavior of the synchronized cells.

For both CDots with or without the serum in media, the amount of internalization by normal HeLa cells was always less than that by the cells at the different phases. A possible explanation is that the synchronized cells were treated with thymidine, which might cause some cell damages.

As a new class of QDs-like nanomaterials, CDots are being

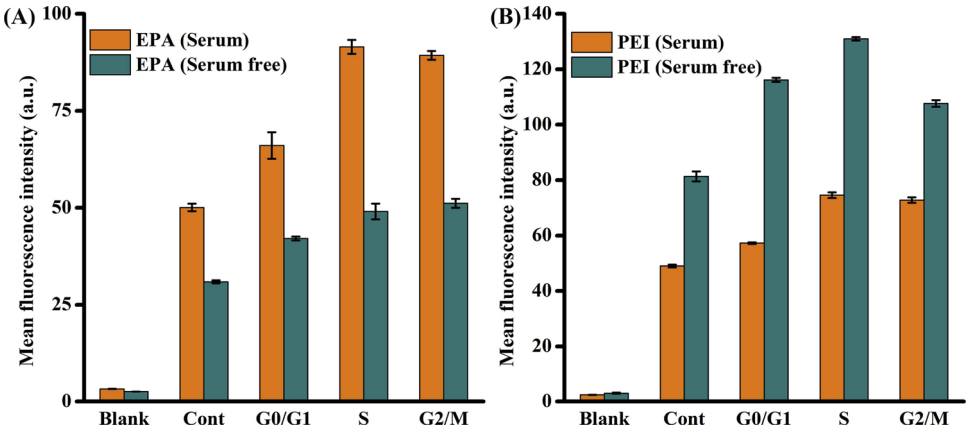

Fig. 4. Flow cytometry results based on the mean fluorescence intensity (MFI) for the uptake of EPA-CDots (A) and PEI-CDots (B) by normal HeLa cells (Cont) and the cells at the indicated different phases. HeLa cells were cultured in culture media with and without serum. Blank presents normal cells without CDots treatments.

considered and developed as versatile platforms for various biomedical applications involving cellular uptakes, such as improved targeting and accumulation of drugs in cells. It is generally understood that the cellular uptake of nanoscale particles or dots varies with their properties such as the size, surface group and surface charge, and also cell parameters such as cell culture conditions and cell line/state [31–33]. The cell-cycle sensitivity may play a major role in determining the cellular uptake of drugs and other biological agents, and consequently dictating many biological effects [34–36]. Therefore, the results on the behaviors of cells in different cycles with respect to their uptake of CDots are valuable to the investigation of dot-cell interactions and to the ongoing effort on developing CDots-based drug delivery systems [34–37].

3.3. Cellular internalization pathways

For an understanding on the cellular uptake of CDots under different conditions, mechanistic issues associated with the uptake of EPA-CDots and PEI-CDots by HeLa cells were explored. Three kinds of endocytosis inhibitors including chlorpromazine hydrochloride (CPZ), nocodazole, and Filipin III were selected for probing contributions of clathrin-mediated endocytosis, macropinocytosis, and caveolin-mediated endocytosis to the cellular uptake of CDots, respectively.

The initial investigation was to determine if the uptake of EPA-CDots by cells was an energy dependent process, and the results were affirmative. As shown in Fig. 5, the cellular uptake of EPA-CDots decreased by about 85% at 4 ℃ in media with/without serum, suggesting an energy-dependent process for the uptake.

Next, the cells were pre-incubated for 30 min with known endocytosis inhibitors, including clathrin-mediated endocytosis (CPZ), caveolae-mediated endocytosis (Filipin III), or macropinocytosis (nocodazole), and then exposed to the CDots for 2 h, and the results are also compared in Fig. 5. In media containing serum, the primary uptake pathway of EPA-CDots was apparently clathrin-mediated endocytosis (Fig. 5A). The caveolae-mediated endocytosis contributed to the cellular uptake as well, especially in cells at the S phase, with an inhibition rate of around 50%. Moreover, there was also macropinocytosis in the cellular uptake by cells at the G_1/G_0 phase, with an inhibition rate of around 13%. In serum-free media on the other hand, clathrin-mediated endocytosis was the most important pathway for cellular uptake of EPA-CDots (Fig. 5B), and unlike in media containing serum caveolae-mediated endocytosis and macropinocytosis only had minor contributions to the cellular uptake.

In similar experiments, the cellular uptake of PEI-CDots was found to be only partially energy dependent. As shown in Fig. 6, the uptake at 4 ℃ was not completely inhibited, suggesting that the HeLa cells took up PEI-CDots in a combination of energy-dependent and non-energy dependent processes. This was different from the uptake of EPA-CDots, for which the non-energy dependent process was less significant, especially in serum-free media.

In serum-containing media, the internalization of PEI-CDots was apparently not affected by nocodazole (Fig. 6), an inhibitor of macropinocytosis. Caveolae-mediated endocytosis and macropinocytosis were responsible for some of the cellular uptake of PEI-CDots. For example, the reduction in cellular uptake was only about 10% in cells at the G_0/G_1 phase after the cells were pretreated with CPZ, an inhibitor of clathrin-mediated endocytosis, suggesting that there must be other internalization pathways for the uptake of PEI-CDots by the cells. In serum-

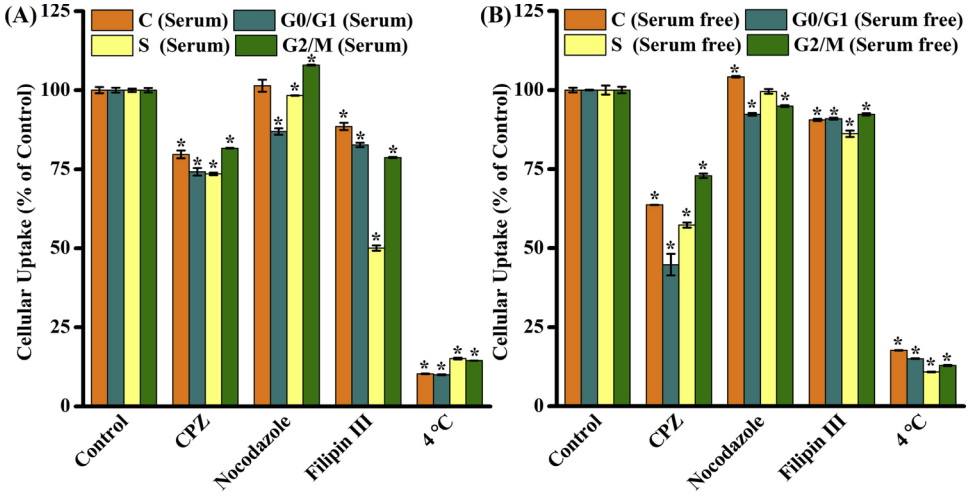

Fig. 5. Mechanisms likely involved in the internalization of EPA-CDots by HeLa cells. (A) For cells cultured in media with serum. (B) For cells cultured in serum-free media. In abscissa, 4 ℃: energy inhibition of cells; CPZ: inhibitor of clathrin-mediated endocytosis; Nocodazole: inhibitor of macropinocytosis; Filipin III: inhibitor of caveolae-mediated endocytosis. $^*p < 0.05$ compared with the control (n = 3).

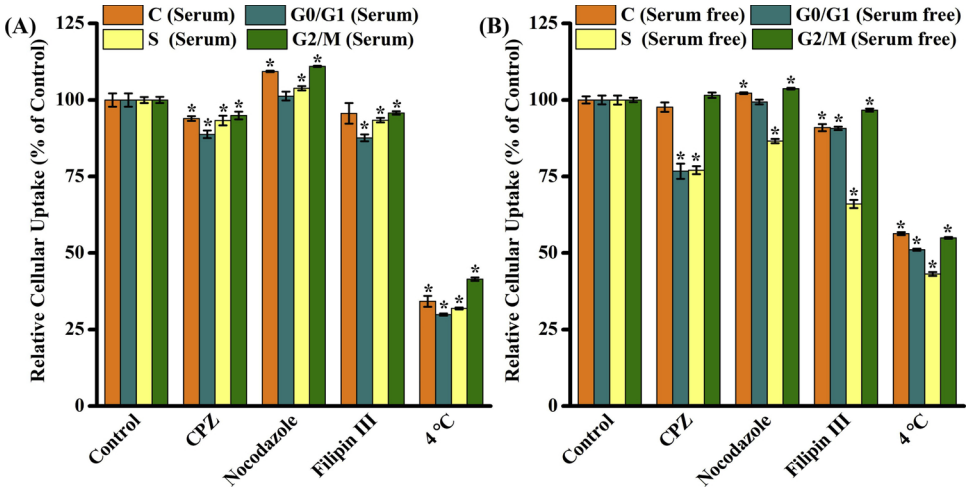

Fig. 6. Mechanisms likely involved in the internalization of PEI-CDots by HeLa cells. (A) For cells cultured in media containing serum. (B) For cells cultured in serum-free media. In abscissa, 4 °C: energy inhibition of cells; CPZ: inhibitor of clathrin-mediated endocytosis; Nocodazole: inhibitor of macropinocytosis; Filipin III: inhibitor of caveolae-mediated endocytosis. $*p <$ 0.05 compared with the control (n = 3).

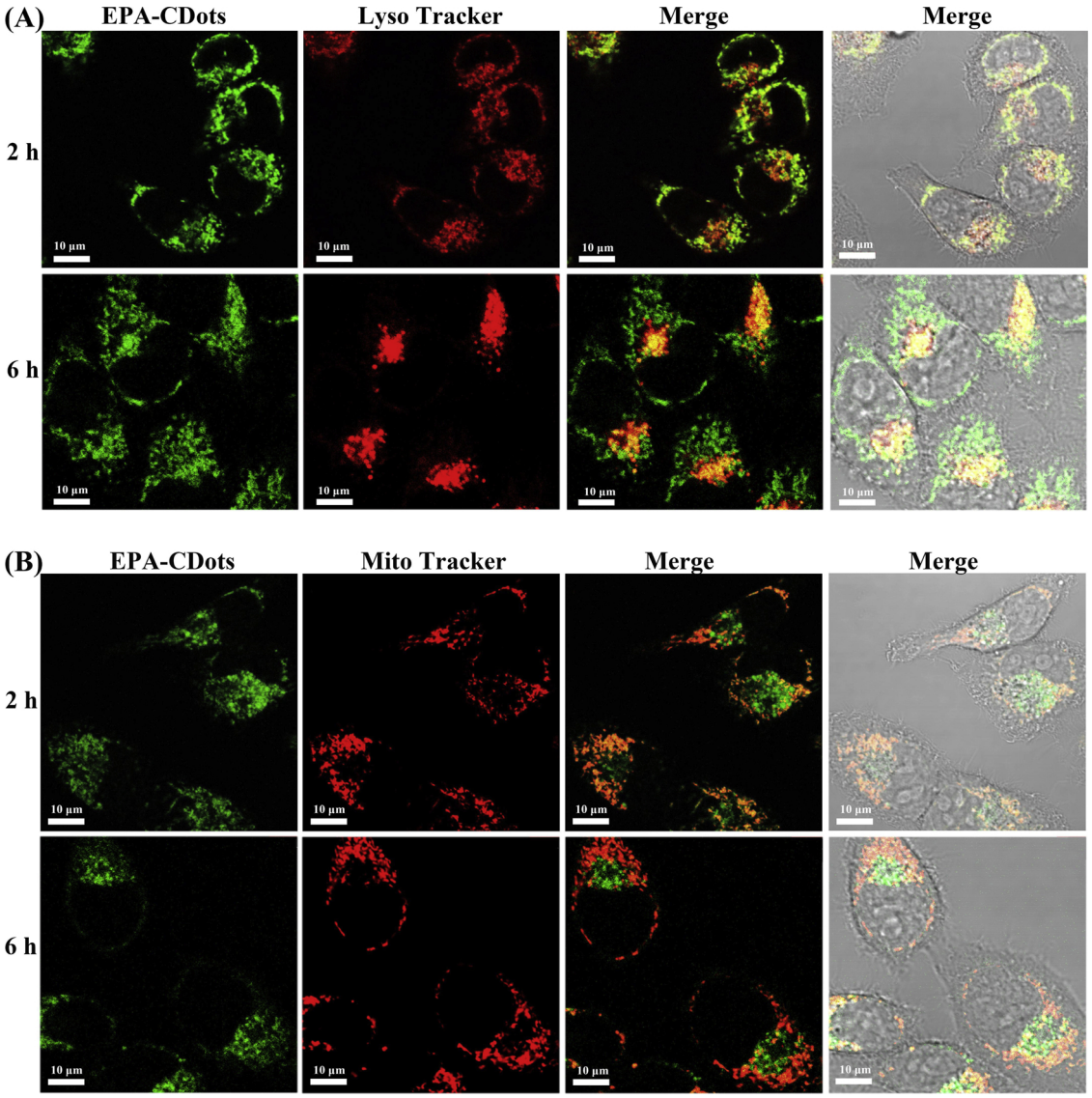

Fig. 7. Confocal fluorescence images of intracellular distribution of EPA-CDots (green color) after incubated with HeLa cells for 2 h and 6 h. (A) Lysosomes were labelled (red color). (B) Mitochondria were labelled (red color). The scales represent 10 μm.

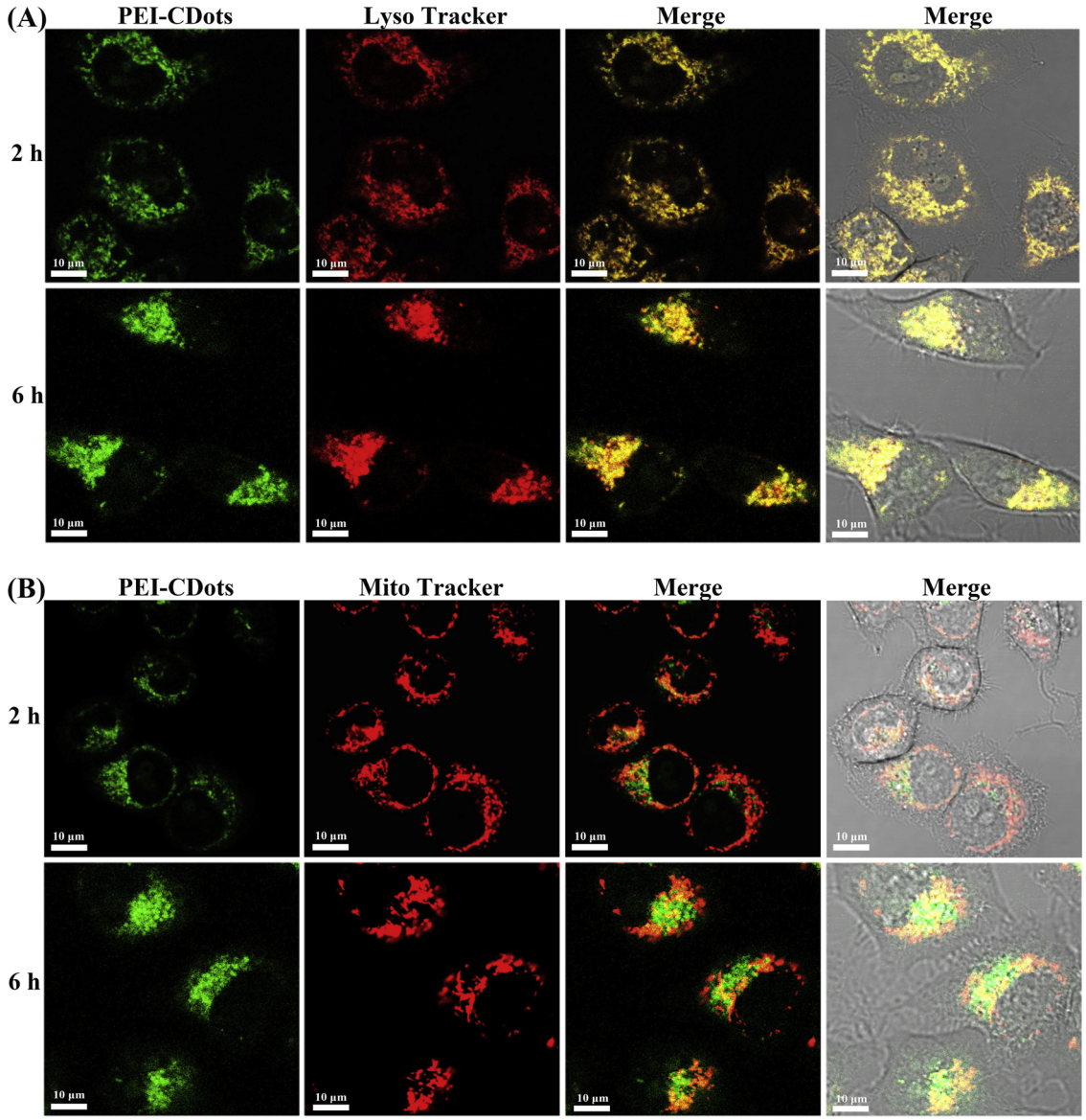

Fig. 8. Confocal fluorescence images of intracellular distribution of PEI-CDots (green color) after incubated with HeLa cells for 2 h and 6 h. (A) Lysosomes were labelled (red color). (B) Mitochondria were labelled (red color). The scales represent 10 μm.

free media, on the other hand, it was found that the uptake of PEI-CDots by the cells at S phase was contributed by all three endocytosis pathways (Fig. 6B). The uptakes by the cells at S phase decreased by about 23% and 34% after the cells were treated with CPZ and Filipin III, respectively. The uptake by the cells at G_0/G_1 phase was due primarily to clathrin-mediated endocytosis, with minor contribution by caveolae-mediated endocytosis. Only caveolae-mediated endocytosis contributed very little to normal cells and cells at G_2/M phase. Obviously, the cell cycle had a complex effect on the internalization of PEI-CDots by the cells.

Cells are typically capable of several forms of endocytosis. The primary mechanism of endocytosis may vary, leading to changes in uptake pathways [38]. For example, endocytosis is suppressed during mitosis, because of the higher tension in cell membrane [39].

3.4. Intracellular localization of CDots

Upon entering cells, nanomaterials are in general transported to different intracellular organelles, where lysosome and mitochondria are the two main locations for the nanomaterials [40,41]. Experimentally, LysoTracker-Red DND-99 and MitoTracker-Red CMXRos were used to label lysosomes and mitochondria, respectively, in HeLa cells for an investigation on the intra-cellular distribution and localization of the CDots.

Fig. 7 shows distributions of EPA-CDots in normal cells after 2 h or 6 h culture. At 2 h, it is clearly that the fluorescence images of EPA-CDots and lysosomes overlapped nicely (Fig. 7A). After 6 h, except for well overlapped fluorescence images of EPA-CDots and lysosomes, there were more EPA-CDots in the cells, consistent with the increased uptake of CDots at a longer culture time. Interestingly, however, the results shown in Fig. 7B suggested that some EPA-CDots were co-localized with mitochondria after incubation for 2 h, but apparently not after 6 h. A logical explanation might be that EPA-CDots could have entered both lysosome and mitochondria in the beginning, and then moved out of mitochondria [42–44]. Similarly for PEI-CDots, fluorescence images of CDots and lysosomes overlapped very well after incubation for 2 h and 6 h (Fig. 8A), but not many CDots in mitochondria (Fig. 8B). The positive charge of PEI-CDots maybe the reason for their lysosome delivery [15,45]. Thus, for PEI-CDots in the cells, their destination was in lysosomes, while lysosome was only one of the destinations for EPA-CDots.

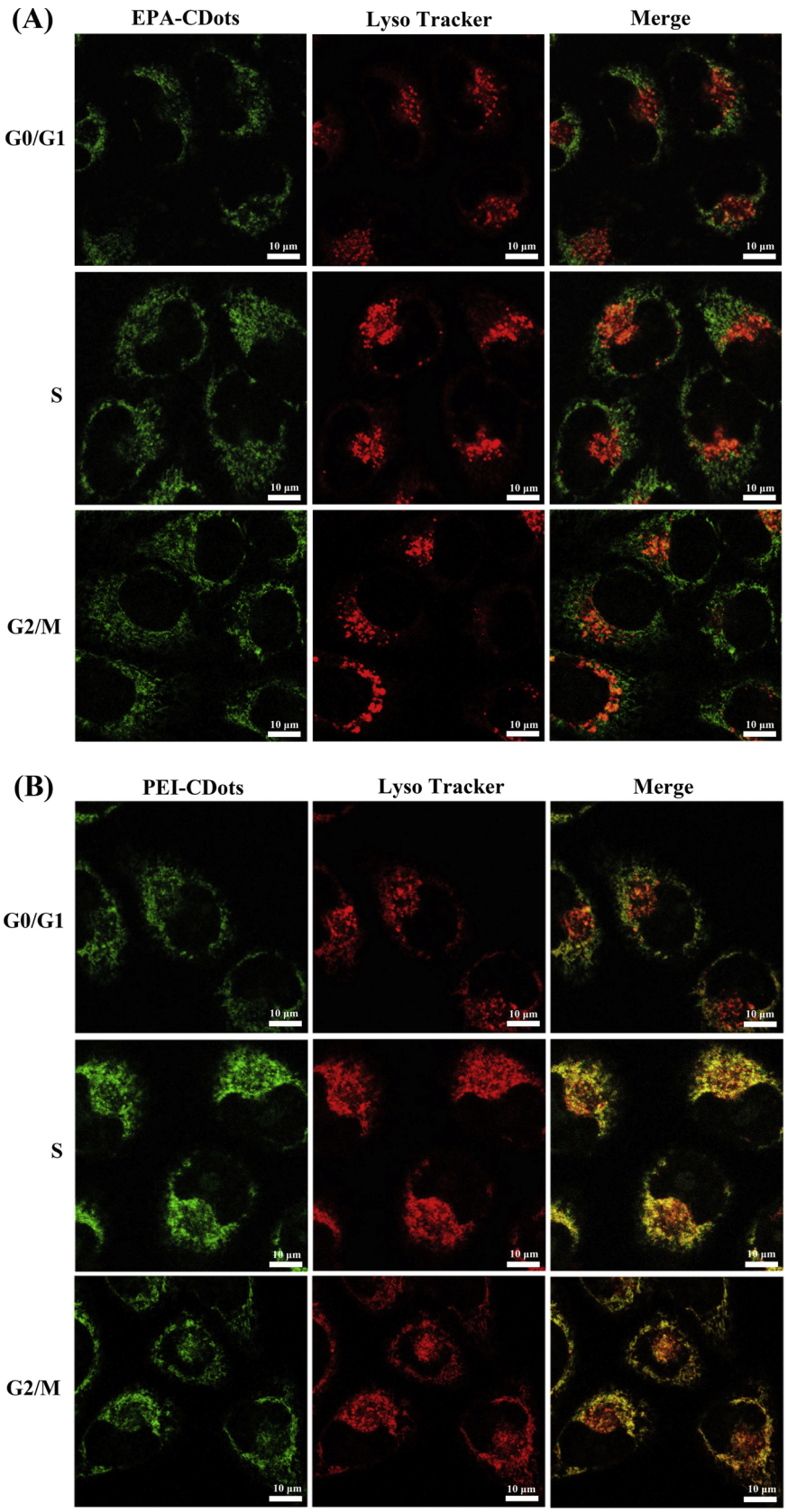

Fig. 9. Confocal fluorescence images of intracellular distribution of EPA-CDots (A) and PEI-CDots (B) after incubated with HeLa cells synchronized at different phases for 2 h. The scales represent 10 μm.

For the cells synchronized at different phases, their fluorescence imaging results post-incubation with EPA-CDots for 2 h are shown in Fig. 9. The fluorescence images of EPA-CDots and lysosomes overlapped much better in cells at S and G_2/M phases than those at G_0/G_1 phase (Fig. 9A), suggesting that more EPA-CDots entered lysosomes of cells at S and G_2/M phases after 2 h incubation. In addition, the fluorescence imaging results confirmed higher uptakes of EPA-CDots by cells at S and G_2/M phases that at G_0/G_1 phase, which is consistent with the flow cytometry results (Fig. 4). Similar to PEI-CDots (Fig. 9B), fluorescence images of PEI-CDots and lysosomes also overlapped much better in cells at S and G_2/M phases than those at G_0/G_1 phase, along with the higher uptakes of PEI-CDots by cells at S phase (Fig. 9B). Thus, it may be concluded that upon the cellular uptake both kinds of CDots entered the lysosomes, regardless of the cell cycle phase.

The results present above show consistent yet complicated dependencies of cellular uptakes of the CDots on not only the dot surface functional groups but also the composition of cell culture medium and more interestingly the cell phase. As reflected by the reports in the literature, the investigations on the development and potential bio-application of CDots have shifted from the simple dot syntheses to the design and preparation of more complex dot structures with multiple moieties for targeting, imaging and therapeutic functions [46]. For example, anticancer drug doxorubicin, 5-fluorouracil, oxaliplatin (Oxa) and cisplatin (IV) prodrug were conjugated with CDots for theranostic uses, and CDots grafted with protophyrin (IX) sensitizer were explored for bioimaging and photodynamic therapy [47–51]. These and other potential applications require a clear understanding of interactions between CDots and cells, including cellular uptake processes, transport and location in cells, etc., which are still in the relatively early stage of exploration. As related in a more specific example, it was reported that the uptake of nanoparticles by tumor cells and the subsequent localization could be achieved by arresting the cells in G_2/M phase using docetaxel in vivo [52]. This suggests opportunities to adjust cells at certain phase to achieve significantly enhanced uptake of CDots, and thus to improve the efficiency in drug delivery and the sensitivity in cell imaging.

4. Conclusions

Cellular uptakes of CDots with two different surface functional groups, EPA-CDots and PEI-CDots, were evaluated using HeLa cells in various cell cycle phases under different cell culture conditions. The internalization pathways of the CDots and their translocations in cells were also investigated. The results indicate that the two CDots have different cell uptake efficiencies, cell internalization pathways and translocations in cells. More specifically, HeLa cells could internalize both CDots by different pathways, with an overall slightly higher internalization efficiency for PEI-CDots. The presence of serum in culture media could have major effects on significantly enhancing the cellular uptake of EPA-CDots, yet markedly inhibiting that of PEI-CDots. The HeLa cells at different cell cycle phases have different behaviors in taking up the CDots, which are also affected by the different dot surface moieties and serum in culture media. Since CDots are being developed for various biomedical applications that are dependent on or dictated by their cellular properties, such as bioimaging, drug delivery and photomediated therapy, the investigation on the cellular behaviors and cellular uptake/translocation mechanisms of CDots will prove valuable information in the design, preparation, manipulation, and uses of CDots for their targeted bio-applications.

Acknowledgments

We thank the National Natural Science Foundation of China (Nos. 31771105, 31871007 and 21701109) and the National Basic Research Program of China (No. 2016YFA0201600) for financial support. The work at Clemson University was supported by a grant from U.S. NSF (1701424).

Appendix A. Supplementary data

Supplementary material related to this article can be found, in the online version, at doi:https://doi.org/10.1016/j.colsurfb.2019.05.027.

References

[1] K.D. Wegner, N. Hildebrandt, Quantum dots: bright and versatile in vitro and in vivo fluorescence imaging biosensors, Chem. Soc. Rev. 44 (2015) 4792–4834.
[2] I.V. Martynenko, A.P. Litvin, F. Purcell-Milton, A.V. Baranov, A.V. Fedorov, Y.K. Gunko, Application of semiconductor quantum dots in bioimaging and biosensing, J. Mater. Chem. B 5 (2017) 6701–6727.
[3] U. Resch-Genger, M. Grabolle, S. Cavaliere-Jaricot, R. Nitschke, T. Nann, Quantum dots versus organic dyes as fluorescent labels, Nat. Meth. 5 (2008) 763–775.
[4] Y.-P. Sun, B. Zhou, Y. Lin, W. Wang, K.A.S. Fernando, P. Pathak, M.J. Meziani, B.A. Harruff, X. Wang, H. Wang, P.G. Luo, H. Yang, M.E. Kose, B. Chen, L.M. Veca, S.-Y. Xie, Quantum-sized carbon dots for bright and colorful photoluminescence, J. Am. Chem. Soc. 128 (2006) 7756–7757.
[5] J.-H. Liu, S.-T. Yang, X.-X. Chen, H. Wang, Fluorescent carbon dots and nanodiamonds for biological imaging: preparation, application, pharmacokinetics and toxicity, Curr. Drug Metab. 13 (2012) 1046–1056.
[6] G.E. LeCroy, S.-T. Yang, F. Yang, Y. Liu, K.A.S. Fernando, C.E. Bunker, Y. Hu, P.G. Luo, Y.-P. Sun, Functionalized carbon nanoparticles: syntheses and applications in optical bioimaging and energy conversion, Coord. Chem. Rev. 320-321 (2016) 66–81.
[7] Z. Peng, X. Han, S. Li, A.O. Al-Youbi, A.S. Bashammakh, M.S. El-Shahawi, R.M. Leblanc, Carbon dots: biomacromolecule interaction, bioimaging and nanomedicine, Coord. Chem. Rev. 343 (2017) 256–277.
[8] L. Cao, M.J. Meziani, S. Sahu, Y.-P. Sun, Photoluminescence properties of graphene versus other carbon nanomaterials, Acc. Chem. Res. 46 (2013) 171–180.
[9] G.E. LeCroy, S.K. Sonkar, F. Yang, L.M. Veca, P. Wang, K.N. Tackett, J.-J. Yu, E. Vasile, H. Qian, Y. Liu, P.G. Luo, Y.-P. Sun, Toward structurally defined carbon dots as ultracompact fluorescent probes, ACS Nano 8 (2014) 4522–4529.
[10] F. Yang, G.E. LeCroy, P. Wang, W. Liang, J. Chen, K.A.S. Fernando, C.E. Bunker, H. Qian, Y.-P. Sun, Functionalization of carbon nanoparticles and defunctionalization — toward structural and mechanistic elucidation of carbon “quantum” dots, J. Phys. Chem. C 120 (2016) 25604–25611.
[11] A. Cao, Z. Ye, Z. Cai, E. Dong, X. Yang, G. Liu, X. Deng, Y. Wang, S.-T. Yang, H. Wang, M. Wu, Y. Liu, A facile method to encapsulate proteins in silica nanoparticles: encapsulated green fluorescence protein as a robust fluorescence probe, Angew. Chem. Int. Ed. 49 (2010) 3022–3025.
[12] P.G. Luo, F. Yang, S.-T. Yang, S.K. Sonkar, L. Yang, J.J. Broglie, Y. Liu, Y.-P. Sun, Carbon-based quantum dots for fluorescence imaging of cells and tissues, RSC Adv. 4 (2014) 10791–10807.
[13] C. Liu, P. Zhang, X. Zhai, F. Tian, W. Li, J. Yang, Y. Liu, H. Wang, W. Wang, W. Liu, Nano-carrier for gene delivery and bioimaging based on carbon dots with PEI-passivation enhanced fluorescence, Biomaterials 33 (2012) 3604–3613.
[14] E. Shuang, Q.-X. Mao, X.-L. Yuan, X.-L. Kong, X.-W. Chen, J.-H. Wang, Targeted imaging of the lysosome and endoplasmic reticulum and their pH monitoring with surface regulated carbon dots, Nanoscale 10 (2018) 12788–12796.
[15] N. Zhou, S. Zhu, S. Maharjan, Z. Hao, Y. Song, X. Zhao, Y. Jiang, B. Yang, L. Lu, Elucidating the endocytosis, intracellular trafficking, and exocytosis of carbon dots in neural cells, RSC Adv. 4 (2014) 62086–62095.
[16] Y. Hu, M.M. Al Awak, F. Yang, S. Yan, Q. Xiong, P. Wang, Y. Tang, L. Yang, G.E. LeCroy, X. Hou, C.E. Bunker, L. Xu, N. Tomlinson, Y.-P. Sun, Photoexcited state properties of carbon dots from thermally induced functionalization of carbon nanoparticles, J. Mater. Chem. C 4 (2016) 10554–10561.
[17] S.-T. Yang, X. Wang, H. Wang, F. Lu, P.G. Luo, L. Cao, M.J. Meziani, J.-H. Liu, Y. Liu, M. Chen, Y. Huang, Y.-P. Sun, Carbon dots as nontoxic and high-performance fluorescence imaging agents, J. Phys. Chem. C 13 (2009) 18110–18114.
[18] J.A. Varela, M.G. Bexiga, C. Aberg, J.C. Simpson, K.A. Dawson, Quantifying size-dependent interactions between fluorescently labeled polystyrene nanoparticles and mammalian cells, J. Nanobiotechnol. 10 (2012) 39.
[19] T. Xia, M. Kovochich, M. Liong, H. Meng, S. Kabehie, S. George, J.I. Zink, A.E. Nel, Polyethyleneimine coating enhances the cellular uptake of mesoporous silica nanoparticles and allows safe delivery of siRNA and DNA constructs, ACS Nano 3 (2009) 3273–3286.
[20] A. Lesniak, F. Fenaroli, M.P. Monopoli, C. Aberg, K.A. Dawson, A. Salvati, Effects of the presence or absence of a protein corona on silica nanoparticle uptake and impact on cells, ACS Nano 6 (2012) 5845–5857.
[21] C. Wilhelm, C. Billotey, J. Roger, J.N. Pons, J.C. Bacri, F. Gazeau, Intracellular uptake of anionic superparamagnetic nanoparticles as a function of their surface coating, Biomaterials 24 (2003) 1001–1011.
[22] S. Zheng, J.-Y. Chen, J.-Y. Wang, L.-W. Zhou, Q. Peng, Effects of cell cycle on the uptake of water soluble quantum dots by cells, J. Appl. Phys. 110 (2011) 124701.
[23] J.A. Kim, C. Aberg, A. Salvati, K.A. Dawson, Role of cell cycle on the cellular uptake and dilution of nanoparticles in a cell population, Nat. Nanotechnol. 7 (2012) 62–68.
[24] J. Tang, Z. Liu, F. Ji, Y. Li, J. Liu, J. Song, J. Li, J. Zhou, The role of the cell cycle in the cellular uptake of folate-modified poly(L-amino acid) micelles in a cell population, Nanoscale 7 (2015) 20397–20404.

[25] G. Hu, X. Cun, S. Ruan, K. Shi, Y. Wang, Q. Kuang, C. Hu, W. Xiao, Q. He, H. Gao, Utilizing G2/M retention effect to enhance tumor accumulation of active targeting nanoparticles, Sci. Rep. 6 (2016) 27669.
[26] S. Patnaik, K.C. Gupta, Novel polyethylenimine-derived nanoparticles for in vivo gene delivery, Exp. Opin. Drug Deliv. 10 (2013) 215–228.
[27] C.W. Evans, M. Fitzgerald, T.D. Clemons, M.J. House, B.S. Padman, J.A. Shaw, M. Saunders, A.R. Harvey, B. Zdyrko, I. Luzinov, G.A. Silva, S.A. Dunlop, K.S. Iyer, Multimodal analysis of PEI-mediated endocytosis of nanoparticles in neural cells, ACS Nano 5 (2011) 8640–8648.
[28] P. Patel, K. Kansara, V.A. Senapati, R. Shanker, A. Dhawan, A. Kumar, Cell cycle dependent cellular uptake of zinc oxide nanoparticles in human epidermal cells, Mutagenesis 31 (2016) 481–490.
[29] O.S. Frankfurt, Increased uptake of vital dye Hoechst 33342 during S phase in synchronized Hela S3 cells, Cytometry 4 (1983) 216–221.
[30] M. Mannisto, M. Reinisalo, M. Ruponen, P. Honkakoski, M. Tammi, A. Urtti, Polyplex-mediated gene transfer and cell cycle: Effect of carrier on cellular uptake and intracellular kinetics, and significance of glycosaminoglycans, J. Gene Med. 9 (2007) 479–487.
[31] M. Zhu, G. Nie, H. Meng, T. Xia, A. Nel, Y. Zhao, Physicochemical properties determine nanomaterial cellular uptake, transport, and fate, Acc. Chem. Res. 46 (2013) 622–631.
[32] S. Zhang, H. Gao, G. Bao, Physical principles of nanoparticle cellular endocytosis, ACS Nano 9 (2015) 8655–8671.
[33] J. Yan, S. Hou, Y. Yu, Y. Qiao, T. Xiao, Y. Mei, Z. Zhang, B. Wan, C.-C. Huang, C.-H. Lin, G. Suo, The effect of surface charge on the cytotoxicity and uptake of carbon quantum dots in human umbilical cord derived mesenchymal stem cells, Colloid Surf. B: Biointerfaces 171 (2018) 241–249.
[34] Y. Shibata, A. Matsumura, F. Yoshida, T. Yamamoto, K. Nakai, T. Nose, I. Sakata, S. Nakajima, Cell cycle dependency of porphyrin uptake in a glioma cell line, Cancer Lett. 129 (1998) 77–85.
[35] R.L. Martin, K.F. Ilett, R.F. Minchin, Cell cycle-dependent uptake of putrescine and its importance in regulating cell cycle phase transition in cultured adult mouse hepatocytes, Hepatology 14 (1991) 1243–1250.
[36] P. Valeriote, L. van Putten, Proliferation-dependent cytotoxicity of anticancer agents: a review, Cancer Res. 35 (1975) 2619–2630.
[37] A.H. Abouzeid, V.P. Torchilin, The role of cell cycle in the efficiency and activity of cancer nanomedicines, Expert Opin. Drug Deliv. 10 (2013) 775–786.
[38] I. Mellman, Endocytosis and molecular sorting, Ann. Rev. Cell Dev. Biol. 12 (1996) 575–625.
[39] D. Raucher, M.P. Sheetz, Membrane expansion increases endocytosis rate during mitosis, J. Cell Biol. 144 (1999) 497–506.
[40] L. Shang, K. Nienhaus, G.U. Nienhaus, Engineered nanoparticles interacting with cells: size matters, J. Nanobiotechnol. 12 (2014) 5.
[41] J. Rejman, M. Nazarenus, D.J. de Aberasturi, A.H. Said, N. Feliu, W.J. Parak, Some thoughts about the intracellular location of nanoparticles and the resulting consequences, J. Colloid Interface Sci. 482 (2016) 260–266.
[42] Y. Han, M. Li, F. Qiu, M. Zhang, Y.-H. Zhang, Cell-permeable organic fluorescent probes for live-cell long-term super-resolution imaging reveal lysosome-mitochondrion interactions, Nat. Commun. 18 (2017) 1307.
[43] Y.C. Wong, D. Ysselstein, D. Krainc, Mitochondria–lysosome contacts regulate mitochondrial fission via RAB7 GTP hydrolysis, Nature 554 (2018) 382–386.
[44] G. Soto-Heredero, F. Baixauli, M. Mittelbrunn, Interorganelle communication between mitochondria and the endolysosomal system, Front. Cell Dev. Biol. 5 (2017) 95.
[45] R. Duncan, S.C. Richardson, Endocytosis and intracellular trafficking as gateways for nanomedicine delivery: opportunities and challenges, Mol. Pharm. 9 (2012) 2380.
[46] M. Hassan, V.G. Gomes, A. Dehghani, S.M. Ardekani, Engineering carbon quantum dots for photomediated theranostics, Nano Res. 11 (2018) 1–41.
[47] Y. Yuan, B. Guo, L. Hao, N. Liu, Y. Lin, W. Guo, X. Li, B. Gu, Doxorubicin-loaded environmentally friendly carbon dots as a novel drug delivery system for nucleus targeted cancer therapy, Colloid Surf. B: Biointerfaces 159 (2017) 349–359.
[48] C. Fowley, N. Nomikou, A.P. McHale, B. McCaughan, J.F. Callan, Extending the tissue penetration capability of conventional photosensitisers: a carbon quantum dot–protoporphyrin IX conjugate for use in two-photon excited photodynamic therapy, Chem. Commun. 49 (2013) 8934–8936.
[49] T. Feng, X. Ai, G. An, P. Yang, Y. Zhao, Charge-convertible carbon dots for imaging-guided drug delivery with enhanced in vivo cancer therapeutic efficiency, ACS Nano 10 (2016) 4410–4420.
[50] M. Zheng, S. Liu, J. Li, D. Qu, H. Zhao, X. Guan, X. Hu, Z. Xie, X. Jing, Z. Sun, Integrating oxaliplatin with highly luminescent carbon dots: an unprecedented theranostic agent for personalized medicine, Adv. Mater. 26 (2014) 3554–3560.
[51] A. Sachdev, I. Matai, P. Gopinath, Carbon dots incorporated polymeric hydrogels as multifunctional platform for imaging and induction of apoptosis in lung cancer cells, Colloid Surf. B: Biointerfaces 141 (2016) 242–252.
[52] H. Gao, G. Hu, Q. Zhang, S. Zhang, X. Jiang, Q. He, Pretreatment with chemotherapeutics for enhanced nanoparticles accumulation in tumor: the potential role of G2 cycle retention effect, Sci. Rep. 4 (2014) 4492.